

Addressing the lattice stability puzzle in the computational determination of intermetallic phase diagrams

Shmuel Barzilai,¹ Cormac Toher,² Stefano Curtarolo,^{2,*} and Ohad Levy^{2,3}

¹*Department of Materials Science, NRCN, P.O.Box 9001, Beer-Sheva 84190, Israel*

²*Department of Mechanical Engineering and Materials Science,
Duke University, Durham, North Carolina 27708, USA*

³*Department of Physics, NRCN, P.O.Box 9001, Beer-Sheva 84190, Israel*

(Dated: October 23, 2021)

The evaluation of phase stabilities of unstable elemental phases is a long-standing problem in the computational assessment of phase diagrams. Here we tackle this problem by explicitly calculating phase diagrams of intermetallic systems where its effect should be most conspicuous, binary systems of titanium with bcc transition metals (Mo, Nb, Ta and V). Two types of phase diagrams are constructed: one based on the lattice stabilities extracted from empirical data, and the other using the lattice stabilities computed from first principles. It is shown that the phase diagrams obtained using the empirical values contain clear contradictions with the experimental phase diagrams at the well known limits of low or high temperatures. Realistic phase diagrams, with a good agreement with the experimental observations, are achieved only when the computed lattice stability values are used. At intermediate temperatures, the computed phase diagrams resolve the controversy regarding the shape of the solvus in these systems, predicting a complex structure with a eutectoid transition and a miscibility gap between two bcc phases.

PACS numbers: 66.70.-f, 66.70.Df

The systematic experimental inspection of thermodynamic properties of alloys is usually based on phenomenological rules and metallurgical experience. It requires considerable efforts commonly associated with melting, casting, heat treatments, homogenization and characterization of series of alloys, which set practical limits on its applicability to a relatively small part of the potential alloy space. Theoretical inspection based on a bottom-up design strategy may enhance the experimental approach, and ultimately replace most of it, by providing rapid computational predictions of structural and thermodynamic properties. The bottom-up strategy becomes viable with the advent of powerful computational methods and available resources. Moreover, the theoretical approach brings a better understanding of alloy design and can reveal shortcuts to achieve the desired alloys as opposed to trial and error methods used in the conventional metallurgical screening.

The fundamental quantity expressing the thermodynamic stability of alloys is the free energy. The free energy of a solid solution phase (ϕ) in a binary system is expressed by

$$G^\phi(x_A, x_B, T) = x_A \cdot {}^0G_A^\phi(T) + x_B \cdot {}^0G_B^\phi(T) + \text{mix}G^\phi(x_A, x_B, T) + \text{ex}G^\phi(x_A, x_B, T), \quad (1)$$

where ${}^0G_A^\phi$ and ${}^0G_B^\phi$ are the Gibbs energies of the pure elements A and B in the ϕ structure, T is the absolute temperature, $\text{mix}G^\phi$ is the mixing energy of the ideal so-

lution

$$\text{mix}G^\phi(x_A, x_B, T) = k_B T (x_A \log x_A + x_B \log x_B) \quad (2)$$

and $\text{ex}G^\phi$ is the excess energy that represents the effects of non-ideality

$$\text{ex}G^\phi = \text{ex}H^\phi + \text{ex}G_{vib}^\phi \quad (3)$$

with

$$\begin{aligned} \text{ex}H^\phi &= H_{AB}^\phi - x_A \cdot H_A^\phi - x_B \cdot H_B^\phi, \quad \text{and} \\ \text{ex}G_{vib}^\phi &= \text{ex}G_{vib,AB}^\phi - x_A \cdot G_{vib,A}^\phi - x_B \cdot G_{vib,B}^\phi. \end{aligned} \quad (4)$$

The phase diagram of an alloy system is determined by evaluating the Gibbs energy difference between its relevant phases, either ordered or disordered. The excess energy is often not available directly from simple experiments, and obtaining it requires considerable effort. It, therefore, usually has to be evaluated computationally. The Gibbs energy difference between the equilibrium and unstable phases of a single element is called *lattice stability*. This quantity is a crucial component in the construction of computational phase diagrams involving elements belonging to different lattice systems, e.g. an hcp-element and a bcc-element. In particular, it presents a conceptual problem in cases where one element is mechanically unstable at low-temperatures in the structure of the other, since the physical meaning of the computed lattice stability is then unclear. This problem has attracted much discussion in the literature, but has yet to be settled [1–9]. It currently presents a major impediment to the development of computational phase diagram databases.

Empirical estimations of lattice stabilities were developed by the Scientific Group Thermodata Europe (SGTE)

* stefano@duke.edu

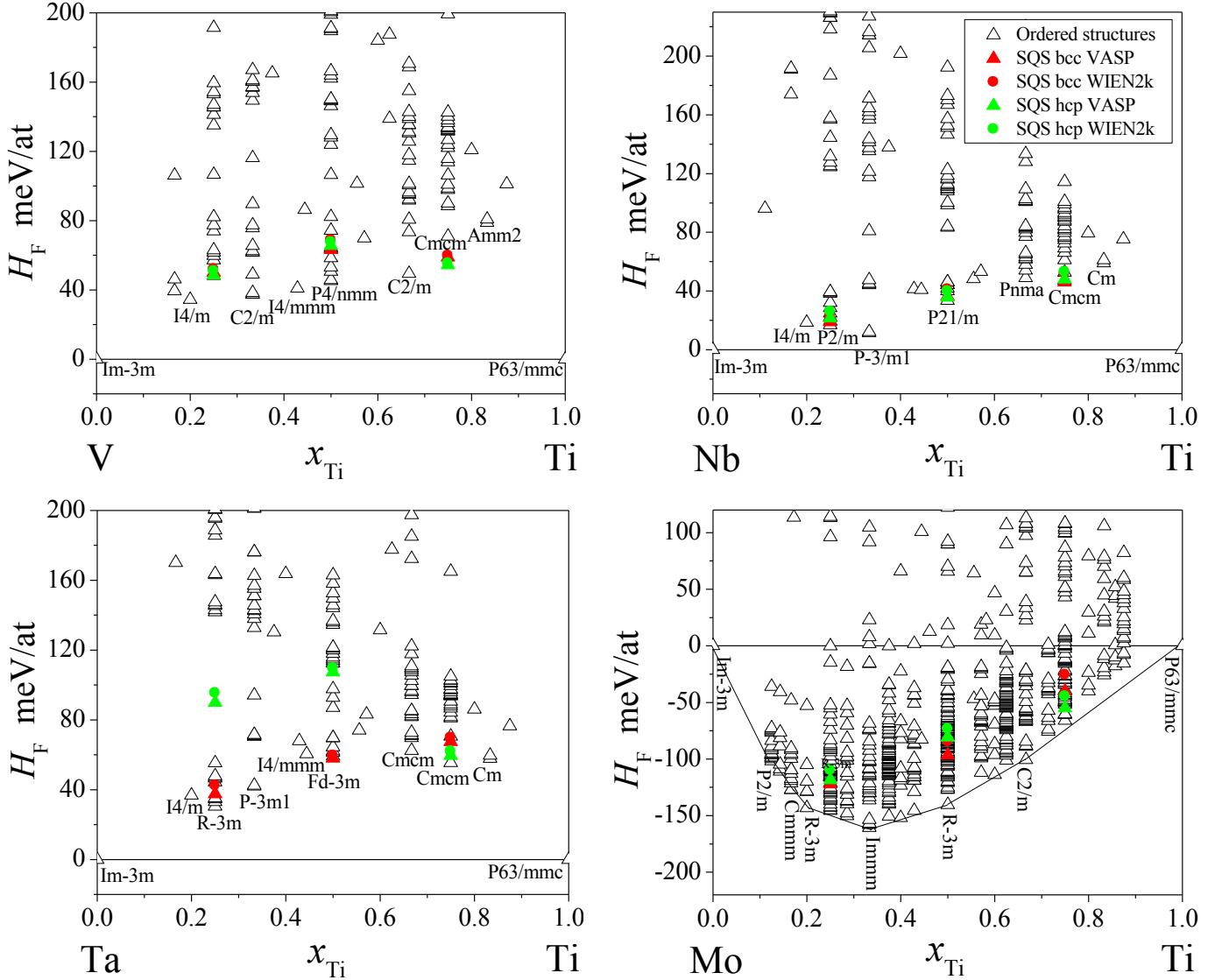


FIG. 1. Formation enthalpy of the lowest lying ordered structures and the bcc- and hcp-SQS computed with respect to the ground states of the respective elements bcc-TM and hcp-Ti.

[10] by direct measurements on pure elements in their stable structures and extrapolations of activity measurements of alloys for the unstable structures. Alternatively, the lattice stability of the pure elements can be easily computed by *ab-initio* methods. Wang *et al.* [4] found a good agreement for the lattice stability between the computed and the empirical estimations for non-transition elements. In these cases, only small differences up to 15 meV/atom were found. However, large discrepancies, most of them in the range of 80-300 meV/atom, were found for the transition metals [2, 5].

Here, we consider these two approaches for assessing lattice stabilities, one empirical and the other computational, aiming to reveal the appropriate approach for constructing the binary phase diagrams of mixed bcc-hcp transition metal systems. We chose four binary systems of the hcp-element titanium, which is well known to be unstable in

the bcc phase at low temperatures, where a bcc solid solution is a prominent feature at higher temperatures over the entire range of compositions. The empirical approach is based on the energies cited in the SGTE database [10]. In the computational approach, these SGTE values are adjusted to reproduce the lattice stabilities computed *ab-initio* for the two elements. These sets are used to construct the TM-Ti (TM=Nb, Mo, V, Ta) binary phase diagrams and thus demonstrate that the development of computational phase diagrams of mixed lattice intermetallic alloy systems requires *ab-initio* based evaluation of the lattice stabilities of their components.

I. RESULTS

To investigate the effect of lattice stability assessment on the predicted phase diagrams, we started by an *ab-initio* screening of ordered stoichiometric structures via the high-throughput framework AFLOW [11, 12]. In addition, the pure elements in the hcp and bcc structures and special quasirandom structures (SQS) for the bcc [13] and hcp [14] structures were computed to estimate the excess formation enthalpies of the corresponding solid solutions.

The *ab-initio* total energy calculations were carried out employing the VASP software within the AFLOW standard for material structure calculations [15]. Complete information about the over 200 ordered structures calculated per system, including initial and relaxed structures and detailed calculation specifications, can be obtained in the open access AFLOWLIB materials data repository [16]. The contribution to the excess Gibbs energy at elevated temperatures, i.e. the vibrational free energy, was considered according to the GIBBS methodology [17, 18] in the quasiharmonic Debye model. The electronic and magnetic excess contributions to the Gibbs energy are expected to be much smaller in these systems and are therefore neglected. The computed excess energies for the two phases were fitted to a sub-subregular model

$${}^{\text{ex}}G = x_{\text{Ta}}x_{\text{Ti}} \left[{}^0L_{\text{TaTi}} + {}^1L_{\text{TaTi}}(x_{\text{Ta}} - x_{\text{Ti}}) + {}^2L_{\text{TaTi}}(x_{\text{Ta}} - x_{\text{Ti}})^2 \right] \quad (5)$$

to retrieve the Redlich-Kister coefficients that describe the excess energy over the entire composition and temperature range. These coefficients were used within the ThermoCalc software [19] to compute two phase diagrams for each binary system, one using the lattice stability of the pure elements taken directly from the SGTE database [10], and the second using the adjusted lattice stability values guided by the *ab-initio* calculations. All total energy calculations were carried out employing the VASP [20] and the WIEN2k [21, 22] software packages.

The high-throughput screening of over 200 structures per system identified no stable structures in the Nb-Ti, V-Ti and Ta-Ti systems, in agreement with the experimental data that includes no intermetallic compounds in these systems. On the other hand, many ordered structures with negative formation enthalpies were found in the Mo-Ti system, of which 6 are identified as potential stable compounds. Figure 1 presents these results for the various ordered structures as well as for the bcc- and hcp-SQS. The complete information about all the structures can be found in the open access AFLOW materials data repository [15, 16, 23].

The Gibbs energy for a specific solid solution structure is obtained from the energies of the pure elements in the same structure, and the corresponding configuration and excess energies (Equation (1)). Figure 2 shows the excess energies of the bcc and hcp structures as a function of alloy composition computed from the DFT total ener-

gies of the pure elements and the SQS. They are fitted to Redlich-Kister polynomials of the fourth degree (Equation (5)) [24] to describe the energies at all compositions as a function of temperature. The DFT results obtained from the VASP and WIEN2k calculations are very close. Both yield strong attraction for the hcp phases, but weaker attractions and in some cases even repulsive interactions for the bcc phases. This picture remains when the contribution of the vibrational energy is taken into account, the excess energies are barely affected in three of the examined systems and only a minor effect emerges in the fourth one. Table I summarizes the interaction energy coefficients between the TM and Ti atoms for both phases, as retrieved from the fitted sub-subregular model.

TABLE I. The Redlich-Kister coefficients obtained for the sub-subregular model of the temperature dependent excess energies of the TM-Ti systems.

system	phase	0L [meV/at]	1L [meV/at]	2L [meV/at]
Mo-Ti	hcp	-1185+0.009T	-1484+0.040T	-1704+0.012T
	bcc	-604.7+0.003T	-147.7+0.004T	-468.6+0.003T
Ti-V	hcp	-254.4-0.002T	705.9-0.020T	-627.6-0.002T
	bcc	34.2+0.003T	-242.1+0.008T	-137.6+0.034T
Nb-Ti	hcp	-454-0.013T	-931+0.028T	-624+0.005T
	bcc	-73.3-0.013T	146-0.006T	-179+0.020T
Ta-Ti	hcp	-133.7-0.081T	-574.4+0.042T	-865.7-0.042T
	bcc	9.7-0.076T	133.1+0.024T	-100.2-0.022T

To construct a full phase diagram, it is important to define correctly the energy of the pure elements in their stable and unstable structures. This is especially important for solid solution systems that display strong attractions in their unstable phase. In our case, strong attractions were computed between the TM and Ti in the hcp phase, thus, erroneous evaluation of the lattice stability may prefer the unstable hcp phase to the stable bcc phase even at the bcc rich side of the phase diagram. To investigate the effect of this choice we considered the two sets of ${}^0G_{\text{TM}}$ and ${}^0G_{\text{Ti}}$ mentioned in the introduction: the empirical set taken directly from the SGTE database, and the computationally guided set where the temperature independent coefficients of the SGTE energies of the unstable phases (hcp-Ta, -Mo, -Nb, -V, and bcc-Ti) were adjusted to reproduce the *ab-initio* computed lattice stabilities. For Ti, the known existence of an hcp-bcc phase transition at 882°C allows us to derive a temperature dependent correction. These adjustments are summarized in Table II.

As can be seen from Table II, both approaches show that the bcc structure is more stable for the TM elements and the hcp structure is more stable for Ti, in agreement with the experimental and computational data [25–27]. However, in all of these cases the stability level computed by the DFT is higher. The difference in lattice stability is quite small for Ti (~ 0.04 eV/at), but significant for the bcc-elements. These differences would be of little effect

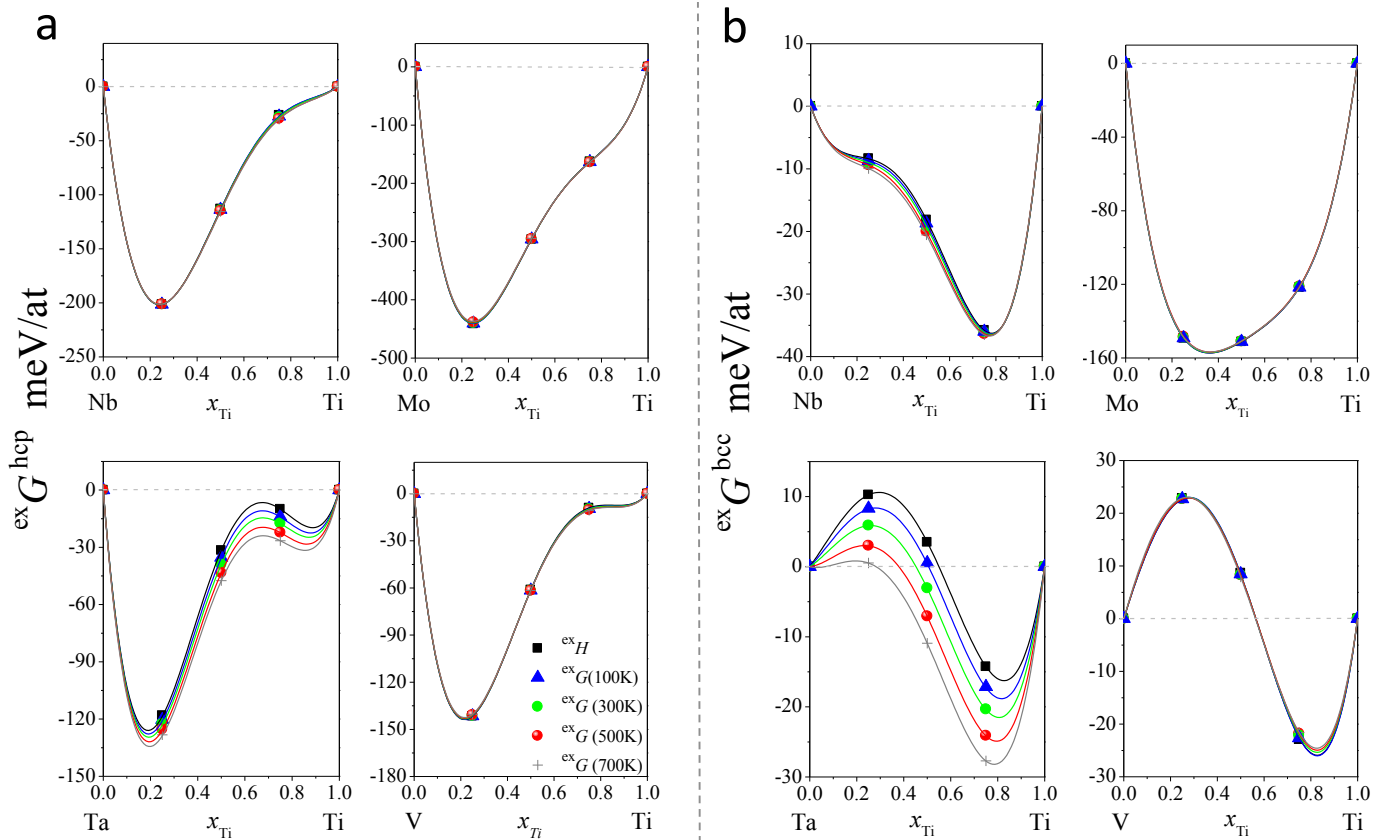


FIG. 2. Excess energies at 0K, ${}^{\text{ex}}H$, and with the finite temperature contributions, ${}^{\text{ex}}G$, computed *ab-initio* by the GIBBS model [18] for the (a) hcp structures and (b) bcc structures. The solid lines represent the fits of the computed points to a sub-subregular model.

TABLE II. The lattice stabilities $\Delta H_{\text{TM}}^{\text{bcc-hcp}}$, of the TM elements (TM = Nb, Mo, V and Ta), and $\Delta H_{\text{Ti}}^{\text{hcp-bcc}}$ as computed from the SGTE values and the DFT calculations. The phase stability adjustments are added to the SGTE values of the ${}^0G_{\text{TM}}$ in the hcp phase and to the ${}^0G_{\text{Ti}}$ in the bcc phase.

elem.	$\Delta H_{\text{TM}}^{\text{bcc-hcp}}$ or $\Delta H_{\text{Ti}}^{\text{hcp-bcc}}$ eV/at (kJ/mol)		Adjustment eV/at (kJ/mol)
	SGTE	DFT	
Ta	-0.124 (-12)	-0.278 (-27)	0.154 (15)
Mo	-0.118 (-11.5)	-0.431 (-41.8)	0.312 (30.3)
Nb	-0.103 (-10)	-0.297 (-28.8)	0.194 (18.9)
V	-0.041 (-4)	-0.253 (-24.6)	0.212 (20.6)
Ti	-0.071 (-6.8)	-0.11 (-10.6)	$0.039 - 3.377 \cdot 10^{-5}T$ (3.8-0.00329T)

in ideal systems, where the attractions between the elements are relatively small. But, as shown in Figure 2, in the cases examined here, the interaction between the TM and Ti is strong, especially in the hcp phase. Figures 3 and 4 show the thermodynamic properties of the TM-Ti systems computed with the empirical set of ${}^0G_{\text{TM}}$

and ${}^0G_{\text{Ti}}$, taken directly from the SGTE (3a and 4a) and with the computationally guided set (3b and 4b). Figure 3 presents the Gibbs energies of the TM-Ti alloys in the hcp and the bcc structures at 882°C. It is well established that above this transition temperature of Ti from hcp to bcc, bcc is the stable phase for the entire concentration range of these alloy systems [26, 28–39]. However, using the SGTE values for ${}^0G_{\text{TM}}$ and ${}^0G_{\text{Ti}}$ we find (Figure 3a) that the hcp solid solutions are more stable than the bcc solutions near 20 at % of Ti. This contradiction disappears using the computationally adjusted ${}^0G_{\text{TM}}$ and ${}^0G_{\text{Ti}}$ (Figure 3b).

The binary phase diagrams for these TM-Ti systems were computed using the Thermo-Calc software, with the excess energies from Table I and the two sets of ${}^0G_{\text{TM}}$ and ${}^0G_{\text{Ti}}$ (Figure 4). Here again, unreasonable results are obtained with the empirical set. As can be seen in Figure 4a, a stable hcp compound emerges around 20 at% of Ti. For the Mo-Ti system, which requires the largest DFT adjustment (addition of 0.312 eV/at to ${}^0G_{\text{Mo}}(\text{hcp})$ of the SGTE) the hcp compound seems to be stable up to 5000°C. Obviously, this result is wrong.

The computational set of ${}^0G_{\text{TM}}$ and ${}^0G_{\text{Ti}}$ leads to realistic results, as shown in Figure 4b. For the Mo-Ti, Ta-Ti and Nb-Ti systems, the computed phase diagrams reproduce the known structural features of the experimental

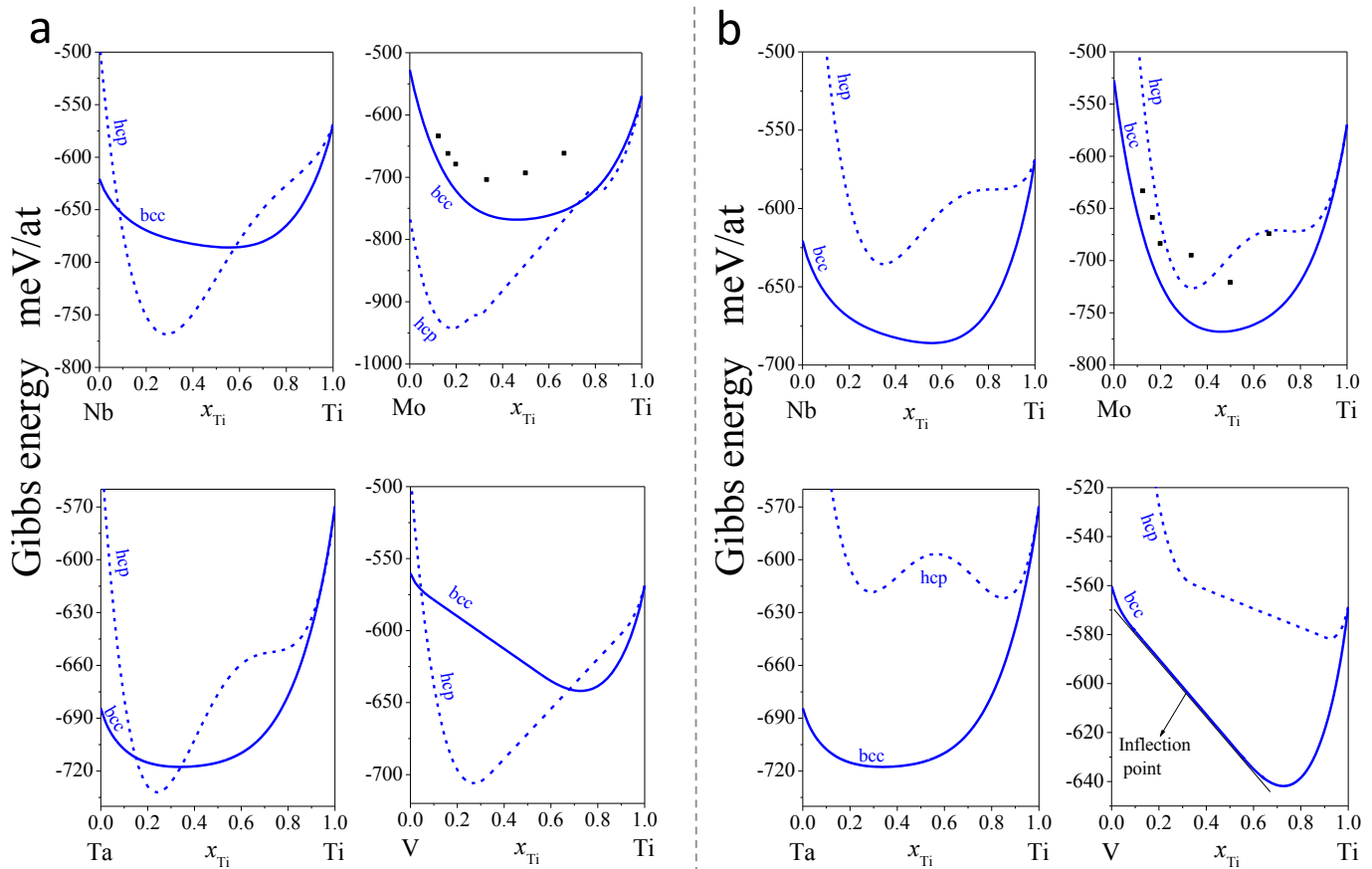


FIG. 3. The computed solid solution Gibbs energies for the hcp (dash lines) and bcc (solid lines) phases in the TM-Ti systems at 882°C, the hcp-bcc transition temperature of titanium; (a) using the empirical set of ${}^0G_{\text{TM}}$ and ${}^0G_{\text{Ti}}$ from the SGTE database, and (b) using the set of DFT adjusted lattice stabilities.

phase diagrams at temperatures above 500°C [29, 30], i.e. a stable bcc solid solution over most compositions and a narrow bcc-hcp phase separation at the Ti-rich side. At low temperatures, the wide bcc-hcp phase separation is also reproduced in the Ta-Ti, Nb-Ti and V-Ti systems, and unobserved new compounds are predicted in the Mo-Ti system below 200°C. These predicted structures likely escaped detection until now due to the slow diffusion toward equilibrium at those low temperatures. At intermediate temperatures, the characteristics of the solvus between the phase separation regime and the solid solution region support those experimental reports [29, 30] that find a phase separation hump between two stable bcc phases defined by monotectoid points. The monotonic solvus reported by other studies [30, 31] should therefore be replaced by this more complex structure.

In the Ti-V system, the predicted bcc phase separation hump has a critical temperature of $\sim 1200^\circ\text{C}$ and a monotectoid temperature at $\sim 200^\circ\text{C}$. One version of the experimental phase diagram shows the same features but with a critical temperature of $\sim 850^\circ\text{C}$ and a monotectoid temperature at $\sim 675^\circ\text{C}$, while another version reports a monotonically decreasing solvus temperature with increasing vanadium concentration [30]. The calculated phase diagram clearly favors the complex solvus structure.

Its features are, however, quite sensitive to the interaction between the pure elements. A reduction of merely 5 meV/at of the attractive and repulsive interactions at 700K would eliminate the inflection point shown in Figure 3b and reduce the critical temperature from 1200°C to the experimental value of 850°C. Such a reduction may be achieved by a more accurate modeling of the vibrational energy, rather than the quasiharmonic Debye model used here.

II. CONCLUSIONS

The determination of phase diagrams requires the evaluation of the free energy differences between multiple phases of elements, compounds and solid solutions based on a few lattices. This requirement leads to the problem of assigning definite values of energy to unstable phases of the constituent elements, which is considered to preclude the direct use of lattice stabilities derived for these structures by *ab-initio* electronic structure calculations. Attempts to resolve this problem, such as the current CALPHAD practice, are usually based on extrapolations that aim to give a smooth continuation of the Gibbs energy through the unstable range of alloy compositions of

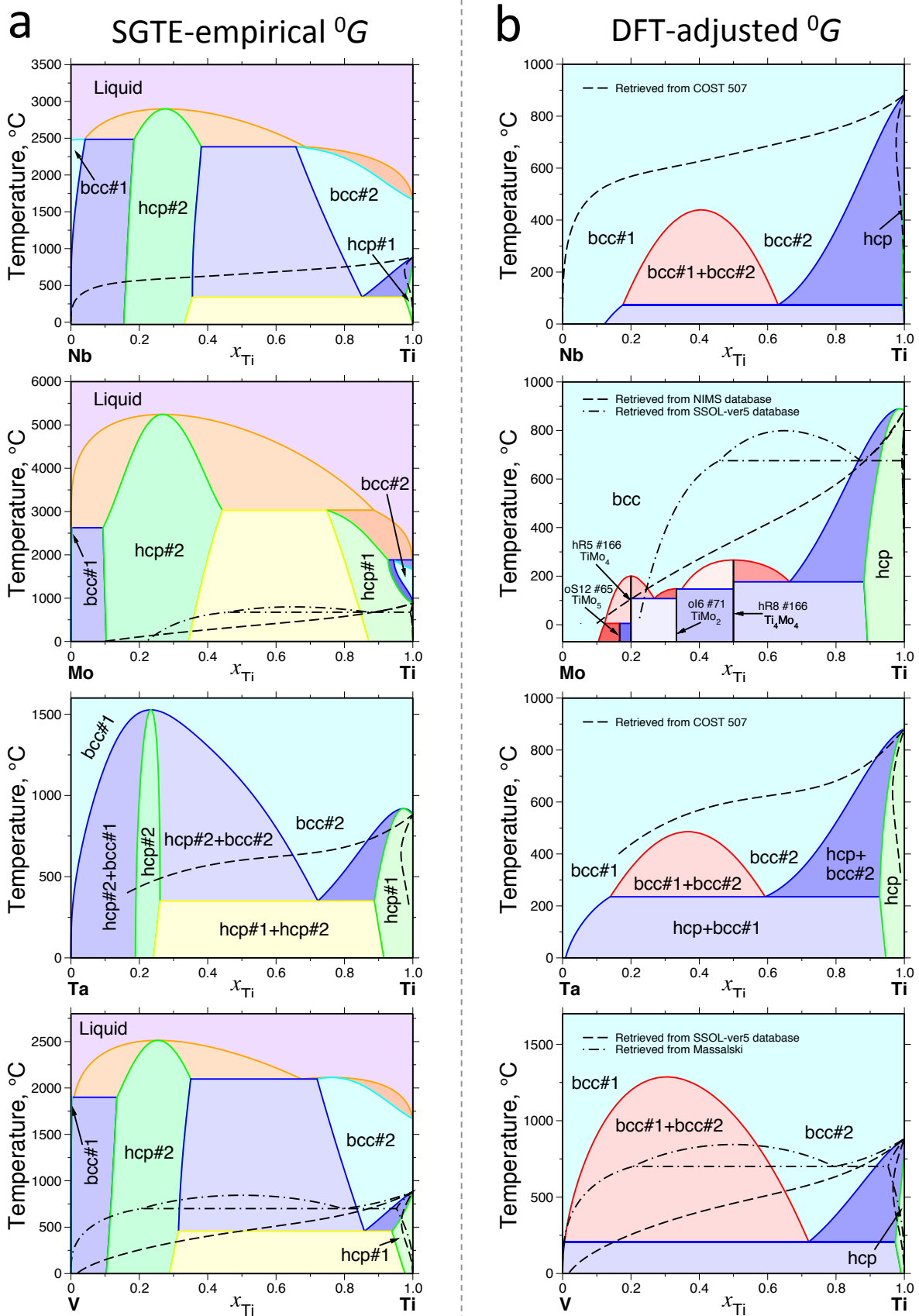


FIG. 4. The computed TM-Ti phase diagrams based on (a) the empirical set of ${}^0G_{\text{TM}}$ and ${}^0G_{\text{Ti}}$ from SGTE database, and (b) DFT adjusted lattice stabilities. The dashed and dotted lines represent experimentally assessed diagrams [30, 31, 38, 39]. DFT adjustment greatly improve predictions with respect to the experimental results.

the investigated system. The assignment of the extrapolation is highly non-unique and is usually regarded as devoid of physical content but merely provides a convenient description of multi-component alloys. Moreover, its consistency with established experimental data cannot be always guaranteed and may lead to errors in the assessment of the phase diagram.

Here, we examine four binary systems of transition metal alloys, TM-Ti systems with TM= Mo, Nb, Ta and V, in which the problem of unstable phases of the elements arises. We assess the phase diagrams of these systems using two approaches for the lattice stabilities of their respective constituents, one in which they are derived from DFT calculations and another where the empirical SGTE values are used without further adjustments. The resulting phase diagrams clearly demonstrate that attempts to mix computational results for the unknown properties of the solid solutions with an empirical assessment of the

lattice stabilities of the elements lead to phase diagrams that badly contradict established experimental data. On the other hand, the use of the *ab-initio* lattice stability values produces phase diagrams that agree well with the available observations and extends them to temperature regimes where experimental data is lacking. In the four cases we examined, it is predicted that the transition from high-temperature solid solutions to low-temperature phase separation is characterized by a complex solvus with a miscibility gap between two bcc phases.

III. ACKNOWLEDGEMENTS

C.T and S.C acknowledge partial support by DOD-ONR (N00014-13-1-0635, N00014-11-1-0136, N00014-09-1-0921). The AFLOW consortium would like to acknowledge the Duke University - Center for Materials Genomics and the CRAY corporation for computational support.

-
- [1] G. Grimvall, B. Magyari-Köpe, V. Ozoliņš, and K. A. Persson, *Lattice instabilities in metallic elements*, Rev. Mod. Phys. **84**, 945–986 (2012).
- [2] P. J. Craievich, M. Weinert, J. M. Sanchez, and R. E. Watson, *Local stability of nonequilibrium phases*, Phys. Rev. Lett. **72**, 3076–3079 (1994).
- [3] A. E. Kissavos, S. Shallcross, V. Meded, L. Kaufman, and I. A. Abrikosov, *A critical test of ab initio and CALPHAD methods: The structural energy difference between bcc and hcp molybdenum*, Calphad **29**, 17–23 (2005).
- [4] Y. Wang, S. Curtarolo, C. Jiang, R. Arróyave, T. Wang, G. Ceder, L.-Q. Chen, and Z.-K. Liu, *Ab initio lattice stability in comparison with CALPHAD lattice stability*, Calphad **28** (2004).
- [5] M. Sluiter, *Ab Initio lattice stabilities of some elemental complex structures*, Calphad **30**, 357–366 (2006).
- [6] V. Ozoliņš, *First-Principles Calculations of Free Energies of Unstable Phases: The Case of fcc W*, Phys. Rev. Lett. **102**, 065702 (2009).
- [7] T. Uesugi, S. Miyamae, and K. Higashi, *Enthalpies of Solution in Ti-X (X=Mo, Nb, V and W) Alloys from First-Principles Calculations*, Materials Transactions **54**, 484–492 (2013).
- [8] M. Palumbo, B. Burton, A. Costa e Silva, B. Fultz, B. Grabowski, G. Grimvall, B. Hallstedt, O. Hellman, B. Lindahl, A. Schneider, P. E. A. Turchi, and W. Xiong, *Thermodynamic modelling of crystalline unary phases*, Phys. Stat. Solidi B **251**, 14–32 (2014).
- [9] A. van der Walle, Q. Hong, S. Kadkhodei, and R. Sun, *The free energy of mechanically unstable phases*, Nat. Commun. **6**, 7559 (2015).
- [10] A. T. Dinsdale, *SGTE Data for Pure Elements*, Calphad **15**, 317 (1991).
- [11] S. Curtarolo, W. Setyawan, G. L. W. Hart, M. Jahnátek, R. V. Chepulskii, R. H. Taylor, S. Wang, J. Xue, K. Yang, O. Levy, M. J. Mehl, H. T. Stokes, D. O. Demchenko, and D. Morgan, *AFLOW: an automatic framework for high-throughput materials discovery*, Comp. Mat. Sci. **58**, 218–226 (2012).
- [12] O. Levy, G. L. W. Hart, and S. Curtarolo, *Uncovering Compounds by Synergy of Cluster Expansion and High-Throughput Methods*, J. Am. Chem. Soc. **132**, 4830–4833 (2010).
- [13] C. Jiang, C. Wolverton, J. Sofo, L. Q. Chen, and Z.-K. Liu, *First-principles study of binary bcc alloys using special quasirandom structures*, Phys. Rev. B **69**, 214202 (2004).
- [14] D. Shin, R. Arróyave, Z. K. Liu, and A. V. de Walle, *Thermodynamic properties of binary hcp solution phases from special quasirandom structures*, Phys. Rev. B **74**, 024204 (2006).
- [15] C. E. Calderon, J. J. Plata, C. Toher, C. Oses, O. Levy, M. Fornari, A. Natan, M. J. Mehl, G. L. W. Hart, M. Buongiorno Nardelli, and S. Curtarolo, *The AFLOW standard for high-throughput materials science calculations*, Comp. Mat. Sci. **108 Part A**, 233–238 (2015).
- [16] S. Curtarolo, W. Setyawan, S. Wang, J. Xue, K. Yang, R. H. Taylor, L. J. Nelson, G. L. W. Hart, S. Sanvito, M. Buongiorno Nardelli, N. Mingo, and O. Levy, *AFLOWLIB.ORG: A distributed materials properties repository from high-throughput ab initio calculations*, Comp. Mat. Sci. **58**, 227–235 (2012).
- [17] M. A. Blanco, E. Francisco, and V. Luaña, *GIBBS: isothermal-isobaric thermodynamics of solids from energy curves using a quasi-harmonic Debye model*, Computer Physics Communications **158**, 57–72 (2004).
- [18] C. Toher, J. J. Plata, O. Levy, M. de Jong, M. D. Asta, M. Buongiorno Nardelli, and S. Curtarolo, *High-Throughput Computational Screening of thermal conductivity, Debye temperature and Grüneisen parameter using a quasi-harmonic Debye Model*, Phys. Rev. B **90**, 174107 (2014).
- [19] J. O. Andersson, T. Helander, L. Höglund, P. Shi, and B. Sundman, *Thermo-Calc & DICTRA, computational tools for materials science*, Calphad **26**, 273–312 (2002).
- [20] G. Kresse and J. Furthmüller, *Efficient iterative schemes for ab initio total-energy calculations using a plane-wave basis set*, Phys. Rev. B **54**, 11169–11186 (1996).

- [21] K. Schwarz, P. Blaha, and G. K. H. Madsen, *Electronic structure calculations of solids using the WIEN2k package for material sciences*, Comput. Phys. Commun. **147**, 71–76 (2002).
- [22] S. Cottenier, *Density Functional Theory and the family of (L)APW-methods: a step-by-step introduction* (Freely available at http://www.wien2k.at/reg_user/textbooks, 2002-2013), 2nd edn.
- [23] R. H. Taylor, F. Rose, C. Toher, O. Levy, K. Yang, M. Buongiorno Nardelli, and S. Curtarolo, *A RESTful API for exchanging Materials Data in the AFLOWLIB.org consortium*, Comp. Mat. Sci. **93**, 178–192 (2014).
- [24] O. Redlich and A. T. Kister, *Algebraic representation of Thermodynamic properties and the classification of solutions*, Ind. Eng. Chem. **40**, 345–348 (1948).
- [25] S. Curtarolo, D. Morgan, and G. Ceder, *Accuracy of ab initio methods in predicting the crystal structures of metals: A review of 80 binary alloys*, Calphad **29**, 163–211 (2005).
- [26] H. Okamoto and K. Cenzual, *Mo-Ti, Ta-Ti, V-Ti and Nb-Ti Phase Diagrams*, in *ASM Alloy Phase Diagrams Database*, <http://www1.asminternational.org/AsmEnterprise/APD>, edited by P. Villars (ASM International, Materials Park, OH, 2006).
- [27] G. L. W. Hart, S. Curtarolo, T. B. Massalski, and O. Levy, *Comprehensive Search for New Phases and Compounds in Binary Alloy Systems Based on Platinum-Group Metals, Using a Computational First-Principles Approach*, Phys. Rev. X **3**, 041035 (2013).
- [28] W. Fuming and H. M. Flower, *Phase separation reactions in Ti-50V alloys*, Materials Science and Technology **5**, 1172–1177 (1989).
- [29] J. L. Murray, *The Mo-Ti (Molybdenum-Titanium) system*, Bulletin of Alloy Phase Diagrams **2**, 185–192 (1981).
- [30] P. Villars, H. Okamoto, and K. Cenzual, *ASM Alloy Phase Diagram Database*: <http://www1.asminternational.org/AsmEnterprise/APD> (2006).
- [31] T. B. Massalski, H. Okamoto, P. R. Subramanian, and L. Kacprzak, eds., *Binary Alloy Phase Diagrams* (American Society for Metals, Materials Park, OH, 1990).
- [32] D. Summers-Smith, *The constitution of tantalum-titanium alloys*, J. Inst. Metals **81** (1952).
- [33] D. J. Maykuth, H. R. Ogden, and R. I. Jaffee, *Titanium-Tungsten and Titanium-Tantalum Systems*, Transactions of the American Institute of Mining and Metallurgical Engineers **192**, 231–237 (1953).
- [34] P. B. Budberg and K. I. Shakova, *Phase Diagram of the Titanium-Tantalum System*, Izv. Akad. Nauk SSSR Neorg. Mat. **3**, 656 (1967).
- [35] P. B. Budberg and K. I. Shakova, *Phase Diagram of the Titanium-Tantalum System*, Inorg. Mater. **3**, 577 (1967).
- [36] European Cooperation in Science and Technology (COST), *507 – Thermochemical database for light metal alloys*, http://www.cost.eu/COST_Actions/mpns/507 (2011).
- [37] D. B. Chernov, V. V. Molokanov, P. B. Budberg, and A. Y. Shinyaev, *Specific features of the interaction between titanium and elements of groups V and VIA of the periodic system, Titanium Alloys*, Proc. Int. Conf. 3rd **2**, 1307–1317 (1982).
- [38] Thermo-Calc Software, *Thermo-Calc Software Database SSOL version 5*, <http://www.thermocalc.com/products-services/software/thermo-calc/> (2015).
- [39] P. Simulation and T. Group, *National Institute for Materials Science, Tsukuba, Ibaraki, Japan*, <http://www.nims.go.jp/cmssc/pst/> (2011).